Spin-orbit coupling in tungsten by spin-polarized two-electron spectroscopy

S. Samarin,[1] O. M. Artamonov,[2] A. D. Sergeant,[1] J. Kirschner,[3] A. Morozov,[3] and J. F. Williams[1]
[1]*Centre for Atomic, Molecular and Surface Physics, University of Western Australia, Perth, WA 6009, Australia.*
[2]*Research Institute of Physics, St. Petersburg University, St. Petersburg, Russia.*
[3]*Max-Planck-Institut für Mikrostrukturphysik, Weinberg 2, D-06120 Halle, Germany.*
(Received 5 April 2004; revised manuscript received 2 June 2004; published 23 August 2004)

We present experimental results on low-energy spin-polarized two-electron spectroscopy of W(100) and W(110). A combination of a coincidence technique with the time-of-flight energy analysis was used to record angular and energy distributions of correlated electron pairs excited by spin-polarized low-energy primary electrons from a single crystal of tungsten. These distributions depend strongly on the polarization and the angle of incidence of the incident electron beam. Experimental data are discussed in terms of the symmetry properties, spin-dependent scattering dynamics, and spin-resolved electronic structure of the sample.

DOI: 10.1103/PhysRevB.70.073403 PACS number(s): 79.20.Kz, 68.49.Jk, 71.70.Ej

INTRODUCTION

Probing the electronic systems of atoms, molecules, and solids by electron impact followed by detection of the scattered electron has become a routine technique for studying the electronic excitation spectrum and secondary emission properties of the system. One of the pathways of the electron interaction with a multielectron system is a binary collision of the incident electron (energy E_o and momentum $\mathbf{K}_o$) with the bound electron (energy E_b) of the target. Detection of two electrons resulting from such a collision extends the scattering picture to a second dimension (with the energies of the two electrons E_1 and E_2) and, by consequence, extends a single electron spectroscopy to a multi- (two-) electron spectroscopy, often referred to as two-electron $(e,2e)$ spectroscopy. In a high-energy limit (10–50 keV primary energy) the cross-section of the $(e,2e)$ scattering is proportional to the momentum density distribution (MDD) of the bound electron.[1] This spectroscopy was applied successfully for studying MDD in atoms, molecules, and thin solid films using the transmission geometry.[1] Application of this technique for surfaces requires low-energy incident electrons and reflection geometry. The capability of grazing angle $(e,2e)$ experiments to map electron momentum distribution in graphite was demonstrated using 300 eV primary electrons and reflection geometry.[2,3] Recently the $(e,2e)$ spectroscopy was adapted for surface studies using low-energy (14–50 eV) primary electrons, backscattering geometry, and time-of-flight energy analysis.[4,5] Experimental[6–8] and theoretical[9–13] works demonstrated the high potential of this technique for studying electron scattering dynamics, surface electronic structure, and electronic correlations.

In the spin-polarized version of this $(e,2e)$ spectroscopy one further dimension is added to the spectra: energy and momentum distributions of correlated electron pairs are measured for two spin-orientations of the incident beam.[14] In general there are two effects that lead to spin-dependent electron scattering from surfaces: the exchange interaction and the spin-orbit interaction. The first is proportional to the scalar product of the average spin of the target and the polarization vector of the incident beam. Therefore it is easily observable in a ferromagnetic surface (where the population of spin-up and spin-down states is unequal) with proper orientation of the magnetization direction and the polarization vector of the electron beam. The application of spin-polarized $(e,2e)$ spectroscopy to a ferromagnetic surface was shown, both theoretically and experimentally, to be very fruitful for studying surface magnetism and spin-dependent scattering dynamics.[15,16] The spin-orbit interaction, in turn, is dominant in the case of a nonmagnetic heavy (large Z) target (tungsten, for example). An extensive theoretical work on spin-polarized low-energy $(e,2e)$ spectroscopy of nonmagnetic surfaces[17] predicted an observable spin-asymmetry in the $(e,2e)$ cross section from tungsten. The collision of an incident electron with a valence electron of the target was treated in a distorted-wave Born approximation formalism with exchange, the four relevant quasi-one-electron states being solutions of the Dirac equation. To obtain detailed insight into the origin of the individual features of the $(e,2e)$ spectra of W(100) and their spin asymmetry, additional calculations were performed where each of the four relevant wave functions were modified artificially such that spin-orbit coupling and elastic scattering amplitudes from ion-core planes were selectively switched off. The calculated spin asymmetry of the $(e,2e)$ cross section on W(100) was found to be due mainly to the spin-orbit coupling in the valence electron states.[17]

EXPERIMENT

We report experimental results on the spin-polarized $(e,2e)$ spectroscopy of W(100) and W(110). The sample was cleaned in vacuum using standard procedure[18] including oxygen treatment at 10^{-7} Torr oxygen pressure and 1400 K sample temperature followed by few high-temperature flashes up to 2300 K. The spin-polarized electron source is based on photoemission from a strained GaAs photocathode activated by Cs and oxygen adsorption[19] that produces a spin-polarized electron beam with the polarization parallel or antiparallel to the momentum of photoelectrons depending on the helicity of the incident light. The degree of polarization is estimated to be about 70%. The polarized beam passes

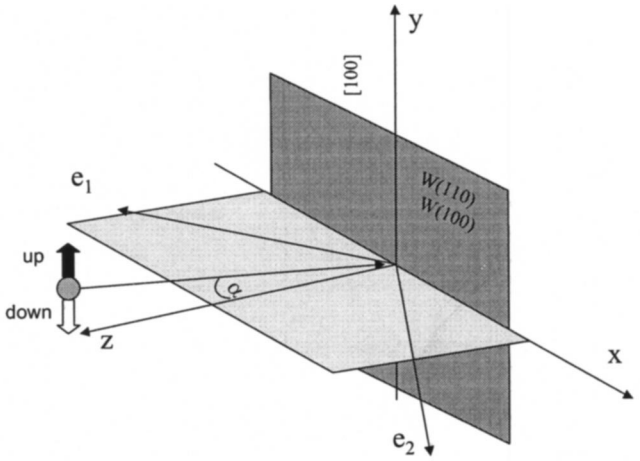

FIG. 1. Geometry of the experiment.

through a 90° electrostatic deflector such that the emergent beam is transversely polarized since the electrostatic field does not affect the spin orientation. The polarization vector can be rotated (up or down polarization) by changing the helicity of the incident light. The polarization direction is chosen perpendicular to the scattering plane containing the incident beam and two detectors. In such a geometrical arrangement one can expect in general a nonvanishing spin-asymmetry in measured spectra because of symmetry considerations.[17] A sketch of the experimental geometry is shown in Fig. 1. The [100] direction of the tungsten crystal is perpendicular to the scattering plane [in both cases of W(100) and W(110)] and the sample can be rotated around this axis varying the angle of incidence α. We use a combination of time-of-flight energy analysis and coincidence technique, which is described elsewhere.[5,20,21] The incident electron beam was pulsed (1 ns pulse width and 2.5×10^6 Hz repetition rate) to have a reference point on the time scale. Position sensitive detectors allow detection of electrons in a wide angular range as well as a flight distance correction for electrons arriving at different locations on the detectors.[21] A correlated electron pair generated by a single incident electron and detected by two detectors is represented by six numbers: arrival times of both electrons T_1 and T_2 and coordinates on the detectors X_1,Y_1,X_2,Y_2, which are stored in a list mode file in the computer. This six-dimensional array [$(e,2e)$ spectrum] for each of the two spin polarizations of the incident beam can be projected on various one- or two-dimensional distributions. As an example of a two-dimensional distribution one can quote the number of correlated pairs as a function of electron energies $I(E_1,E_2)$. For a given primary energy and fixed experimental geometry the $(e,2e)$ spectrum was measured for spin-up (I^+) and spin-down (I^-) polarization of the incident beam and then these two spectra were compared in terms of their difference and spin-asymmetry. To avoid the influence of the incident electron current drift or the sample surface modification (contamination) on the spin-asymmetry during the measurements we altered the polarization of the beam every 5 s and the $(e,2e)$ spectra were measured for spin-up and spin-down polarization of the incident beam. Since the accumulation of data with satisfactory statistics takes approximately 30 h we stopped measurements every few hours and cleaned the sample by a high temperature flash to remove adsorbed residual gases even though the base pressure was in the 10^{-11} Torr range.

RESULTS AND DISCUSSION

Energy and momentum conservation laws of the $(e,2e)$ reaction imply that the valence electron involved in the collision with a projectile can be localized in energy-momentum space. In a single electron collision of the incident electron with a valence electron the energy of the primary electron E_0 and two outgoing electrons E_1,E_2 define the binding energy of the valence electron: $E_b=E_1+E_2-E_0$. The number of cor-

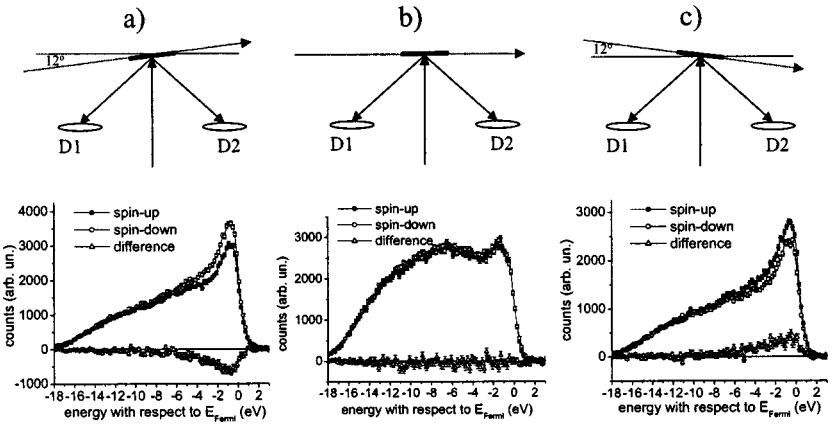

FIG. 2. Binding energy spectra of W(110) recorded at three positions of the sample and primary electron energy 25.5 eV.

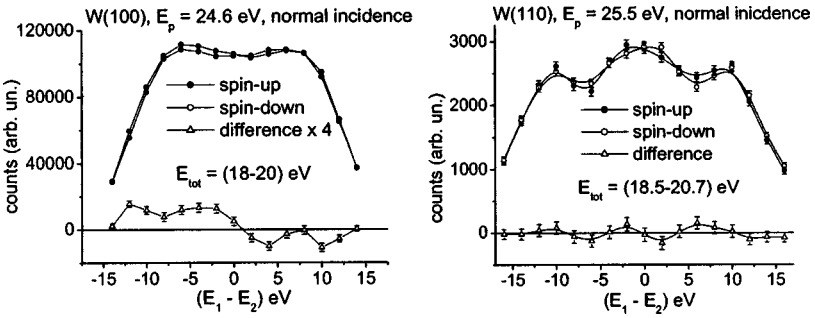

FIG. 3. Energy sharing distributions of correlated electron pairs from W(100) and W(110) recorded at normal incidence.

related electron pairs as a function of the total (sum) energy $E_{\mathrm{tot}}=E_1+E_2$ then represents the "total energy distribution" or as a function of the binding energy, a "binding energy spectrum." For a fixed total energy the two electrons of the pair can share this energy in different ways depending on the scattering dynamics and electronic properties of the surface. The number of electron pairs as a function of the difference energy (E_1-E_2) presents an "energy sharing distribution" for a given total energy, or within a narrow band of total energy. In the case of a crystal surface, the parallel-to-the-surface component of the electron momentum is a good quantum number for four relevant electronic states of the scattering event. Therefore $\mathbf{K}_{o\|}+\mathbf{K}_{b\|}=\mathbf{K}_{1\|}+\mathbf{K}_{2\|}$, where $\mathbf{K}_o$, $\mathbf{K}_b$, $\mathbf{K}_1$, and $\mathbf{K}_2$ are the momenta of the incident, bound, first- detected, and second-detected electrons, respectively. Hence we can present our measured spin-polarized $(e,2e)$ spectra as projections on the binding energy, on $\boldsymbol{K}_{b\|}$, or as energy sharing distributions within a certain total energy band.

Figure 2 represents binding energy spectra measured at 25.5 eV primary energy for three different positions of the sample: normal incidence (panel b) and two off-normal (panels a and c). The angle of incidence was changed by rotating the sample around the axis perpendicular to the scattering plane by ±12°. We note that the shape of the binding energy spectrum depends on the incident angle. At normal incidence there are two maxima in the spectrum: one at about 1 eV below the Fermi level and the second at about 7 eV below the Fermi level. In contrast, for both off-normal (±12°) positions of the sample the binding energy spectrum contains a single pronounced maximum located at 1 eV below the Fermi level. Regarding the spin dependence the normal incidence spectra (panel b) for "spin-up" and "spin-down" primary beams are identical and the difference spectrum is zero. For off-normal incidence the "spin-up" and "spin-down" spectra are different for both positions (a) and (c) and difference spectra have opposite signs: negative for the sample position (a) and positive for the position (c). The difference between spin-up- and spin-down spectra is located in the energy range within a few eV below the Fermi level. It was shown[21,22] that in this energy range the major contribution to the $(e,2e)$ spectrum comes from the two-electron binary collisions whereas for lower energies the contribution from multistep collisions is substantial. Therefore we analyze how two correlated electrons share energy within 2 eV total (binding) energy just below the Fermi level.

For normal incidence the energy sharing distributions from W(100) and W(110) are shown in Fig. 3. We note first that the shape of the distribution for W(100) is different from those for W(110). Secondly, the difference between spin-up and spin-down spectra for both faces of the tungsten crystal exhibits an interesting symmetry feature. Mirror reflection with respect to the $E_1-E_2=0$ point transforms I^+ almost perfectly into I^- and hence changes the sign of the difference spectrum. This is consistent with the theoretical prediction[17] and can be understood from the symmetry analysis of the experimental geometry (Fig. 1). Reflection at the (y,z)-plane reverses the spin of the incident electron (because the spin is an axial vector) and interchanges the two outgoing electrons. It implies that $I^+(E_1-E_2)=I^-(E_2-E_1)$.

When the incidence angle changes from zero to +12° or to −12° the energy sharing distributions change dramatically, both in shape and in spin-dependence (Fig. 4). For normal incidence the distribution is symmetric with respect to the zero point where $E_1=E_2$. For off-normal incidence (panels a and c) the distributions are not symmetric relative to the zero point. For the sample position (a) there is a maximum at

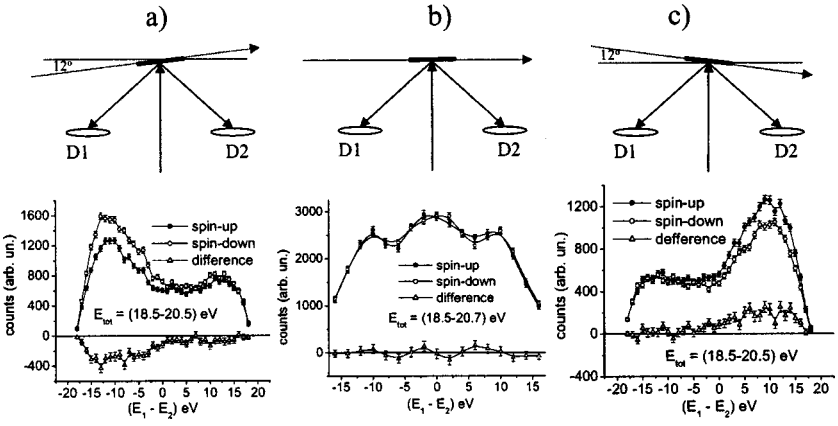

FIG. 4. Energy sharing distributions of correlated electron pairs excited by 25.5 eV primary electrons from W(110) at three different positions of the sample.

$E_1-E_2=-10$ eV whereas for the position (c) the maximum is located at $E_1-E_2=10$ eV. If we take the medium total energy $E_{tot}=19.5$ eV, then the two maxima correspond to the following combinations of electron energies: ($E_1=4.75$ eV; $E_2=14.75$ eV) for the sample position (a) and ($E_1=14.75$ eV; $E_2=4.75$ eV) for the sample position (c). The combinations of momenta would be ($K_1=1.12\text{Å}^{-1}$, $K_2=1.97\text{Å}^{-1}$) and ($K_1=1.97\text{Å}^{-1}$, $K_2=1.12\text{Å}^{-1}$), respectively. Assuming for the sake of simplicity that electrons are detected in the centers of the detectors, the total momentum of the pair would be close to the direction of the specularly reflected primary beam. This means simply that the total momentum of the pair carries the parallel component of the incident electron momentum because of the momentum conservation law. It is interesting to note that the average coincidence count rate for off-normal incidence is about two times higher than for normal incidence. Together with the arguments presented in the discussion of the binding energy spectra for normal and off-normal incidence this indicates that the off-normal incidence is more favorable for observing correlated two-electron emission resulting from the binary collision of the incident electron with the valence electron. Regarding the spin-dependence, one can see that the sharing distributions for off-normal incidences exhibit large differences between spin-up and spin-down spectra. The difference spectra possess broad maxima located at $(E_1-E_2)=-10$ eV for positions (a) and at $(E_1-E_2)=10$ eV for position (c). The asymmetry $A=(I^+-I^-)/(I^++I^-)$ reaches –10% and 10%, respectively. The I^+ and I^- spectra and difference spectrum $D=(I^+-I^-)$ show again an interesting symmetry property. Let us denote by I_a and I_c spectra recorded at geometry (a) and geometry (c), respectively. Reflection at the (y,*z*)-plane reverses the spin of the primary electron and transforms the geometry (a) into geometry (c) with interchange of the outgoing electrons. It implies that $I_a^+(E_1-E_2)=I_c^-(E_2-E_1)$ and, by consequence, $D_a(E_1-E_2)=-D_c(E_2-E_1)$. Comparing the spectra in panels (a) and (c) one can see that difference spectra exhibit such a symmetry.

The origin of the spin-dependence in the $(e,2e)$ spectra, as pointed out,[17] is the spin-orbit coupling in at least one of the four relevant electron states: incident electron state, two outgoing electron states, and a valence electron state. The contribution of each of them to the observed spin-asymmetry can be revealed by a comparison of the measured spectra at different geometries with the appropriate calculations.

SUMMARY

We observed spin-orbit coupling in the inelastic scattering channel of low energy electrons from W(100) and W(110) using spin-polarized $(e,2e)$ spectroscopy. The qualitative agreement of the experimental data with theoretical predictions suggests that this technique can be used for studying spin-dependent electron scattering dynamics from heavy metals as well as spin-related features of their electronic band structure.

ACKNOWLEDGMENTS

We thank S. Key, G. Light (UWA), and H. Engelhard (MPI) for their technical support. One of the authors (O.M.A.) is grateful to the Russian Universities program (Project ur.01.01.040) for financial support.

[1] E. Weigold and Ian E. McCarthy, *Electron Momentum Spectroscopy* (Kluwer Academic/Plenum, New York, 1999).
[2] S. Iacobucci, L. Marassi, R. Camilloni, S. Nannarone, and G. Stefani, Phys. Rev. B **51**, 10 252 (1995).
[3] S. Rioual, S. Iacobucci, D. Neri, A. S. Kheifets, and G. Stefani, Phys. Rev. B **57**, 2545 (1998).
[4] J. Kirschner, O. M. Artamonov, and A. N. Terekhov, Phys. Rev. Lett. **69**, 1711 (1992).
[5] J. Kirschner, O. M. Artamonov, and S. N. Samarin, Phys. Rev. Lett. **75**, 2424 (1995).
[6] S. Samarin, J. Berakdar, O. Artamonov, H. Schwabe, and J. Kirschner, Surf. Sci. **470**, 141 (2000).
[7] J. Berakdar, S. N. Samarin, R. Herrmann, and J. Kirschner, Phys. Rev. Lett. **81**, 3535 (1998).
[8] S. Samarin, R. Herrmann, H. Schwabe, and O. Artamonov, J. Electron Spectrosc. Relat. Phenom. **96**, 61 (1998).
[9] A. S. Kheifets, S. Iacobucci, A. Ruocco, R. Camilloni, and G. Stefani, Phys. Rev. B **57**, 7360 (1998).
[10] H. Gollisch, D. Meinert, Xiao Yi, and R. Feder, Solid State Commun. **102**, 317 (1997).
[11] H. Gollisch, T. Scheunemann, and R. Feder, Solid State Commun. **117**, 691 (2001).
[12] J. Berakdar and M. P. Das, Phys. Rev. A **56**, 1403 (1997).
[13] R. Feder, and H. Gollisch, Solid State Commun. **119**, 625 (2001).
[14] S. N. Samarin, J. Berakdar, O. Artamonov, and J. Kirschner, Phys. Rev. Lett. **85**, 1746 (2000).
[15] A. Morozov, J. Berakdar, S. N. Samarin, F. U. Hillebrecht, and J. Kirschner, Phys. Rev. B **65**, 104425 (2002).
[16] S. Samarin, O. Artamonov, J. Berakdar, A. Morozov, and J. Kirschner, Surf. Sci. **482** (Part 2), 1015 (2001).
[17] H. Gollisch, Xiao Yi, T. Scheunemann, and R. Feder, J. Phys.: Condens. Matter **11**, 9555 (1999).
[18] R. Cortenraada, S. N. Ermolov, V. N. Semenov, A. W. Denier van der Gon, V. G. Glebovsky, S. I. Bozhko, and H. H. Brongersma, J. Cryst. Growth **222**, 154 (2001).
[19] D. T. Pierce, R. J. Celotta, G.-C. Wang, W. N. Unertl, A. Galejs, C. E. Kuyatt, and S. R. Mielczarek, Rev. Sci. Instrum. **51**, 478 (1980).
[20] S. N. Samarin, O. M. Artamonov, D. K. Waterhouse, J. Kirschner, A. Morozov, and J. F. Williams, Rev. Sci. Instrum. **74**, 1274 (2003).
[21] O. M. Artamonov, S. N. Samarin, and J. Kirschner, Appl. Phys. A: Mater. Sci. Process. **A65**, 535 (1997).
[22] R. Feder, H. Gollisch, D. Meinert, T. Scheunemann, O. M. Artamonov, S. N. Samarin, J. Kirschner, Phys. Rev. B **58**, 16 418 (1998).